ARMA 20–2019

Observation of strain localization by digital image correlation to study the influence of particle size distribution

Rattez, H., Veveakis, M. and Mielniczuk B.
Duke university, Durham, NC, USA
Shi, Y.
Wuhan university, Wuhan, China
Sac-Morane, A. and Klaeylé, T.
Ecole Normale Supérieure Paris Saclay, Cachan, France

ABSTRACT: Strain localization is a pervasive phenomenon observed in many materials and characterized by a loss of homogeneity of the field of deformation. In the particular case of geomaterials, this feature often occurs in the form of shear bands observed on outcrops or accompanying the failure of cavities, landslides or fault zones. The characterization of the size of the zone where most of the deformation concentrates is therefore a key parameter to the design of geostructures and the understanding of many natural hazards. It influences also the strength weakening of the material and many multi-physical processes as it affects the temperature increase or the pore pressure evolution. In this study, we focus on the characterization of the influence of the microstructure size on the shear band thickness. Triaxial experiments have been conducted on a silicate sand presenting different particle size distributions: graded and uniform. The shear band thickness evolution is estimated by Digital Image Correlation (DIC) using cameras placed around the triaxial cell. From the field of deformation, a gaussian distribution has enabled to fit the data satisfactorily. The width of the shear band exhibits a rapid decrease until reaching a residual value depending only on the mean grain size.

1. INTRODUCTION

Shear banding is one of the major modes of failure in geomaterials. In particular, it is observed during catastrophic landslides (Segui, Rattez, and Veveakis 2019; Vardoulakis 2002; Veveakis, Vardoulakis, and Di Toro 2007), seismic slips (Rattez et al. 2018b; Rattez, Stefanou, and Sulem 2018; Rice 2006) or around excavated tunnels (Hu et al. 2017) involving mechanisms that occur at several length and time scales. Field observations attest that the width of the band where the shear deformation localizes is narrow, i.e. of millimetric scale or even thinner. Strain localization in narrow bands can be seen as a bifurcation from the homogeneous deformation solution of the underlying mathematical problem (Hill 1962; Rudnicki and Rice 1975; Vardoulakis and Sulem 1995), which is favored by softening behavior of the material. Mechanical processes (e.g. grain crushing, reduction of internal friction etc.), thermal effects, chemical reactions (e.g. dissolution, dehydration etc.) can induce a softening behavior. The characterization of the size of the zone where most of the deformation concentrates is a key parameter to model and predict the mechanical behavior of geomaterials.

Many experimental studies have investigated the mechanism of strain localization using different methods of observation like photogrammetry (Desrues and Viggiani 2004), strain markers (Rathbun and Marone 2010; Smith, Nielsen, and Di Toro 2015), X-ray microtomography with digital volume or image correlation (Desrues et al. 2018; Louis, Wong, and Baud 2007; Takano et al. 2015), microscopy on specimen's slices (Smith, Nielsen, and Di Toro 2015), and digital image correlation from pictures taken by cameras (Bhandari, Powrie, and Harkness 2012; Dautriat et al. 2011; Rechenmacher 2006; Rechenmacher and Finno 2004; Zhang et al. 2014). We can differentiate these observational methods into two subsets: the observation of a variation of a property like the displacement of a marker or a porosity variation after the mechanical loading, or by estimating the increment of deformation following local patterns identified on a picture or scan of the sample. The latter approach is more accurate as it enables to obtain an evolution of the strain localization process during a mechanical loading. Most of the results in the literature for geomaterials were obtained for granular materials presenting a uniform grain size distribution. However, more complex particle distributions can be observed in nature as phenomena like grain breakage or dissolution can affect the grain size distribution (Rattez et al. 2019; Rattez and Veveakis 2020). In particular, The phenomenon of grain breakage can be triggered for quite low stress in the case of carbonate sands (Coop et al. 2004). Several studies have focused on the evolution of particle size distribution and it has been observed that the distribution tend to a final one that is called fractal and present particles with a wide range of diameters. Therefore, a wide distributions of grain sizes is a common feature in fault zones, landslides or at the tip of piles during penetration for example.

In order to investigate the influence of grain size and of the broadness of the grain size distribution on the shear band thickness, we have performed triaxial experiments on granular materials presenting uniform and graded particle distributions. We have observed the evolution of the shear band thickness using Digital Image Correlation from the pictures of three cameras placed at different angles around the triaxial apparatus. From the field of deformation, the shear band can be captured. The width of the shear band exhibits a decrease during the mechanical weakening of the specimen until reaching a residual value.

2. EXPERIMENTAL SETUP

2.1. Materials

Triaxial experiments have been conducted on dry silica sand samples. This sand is usually used for concrete and presents a graded distribution. The initial distribution has been modified to extract uniform distributions or graded distributions with different mean grain sizes using sieves following the American standard ASTM D422.

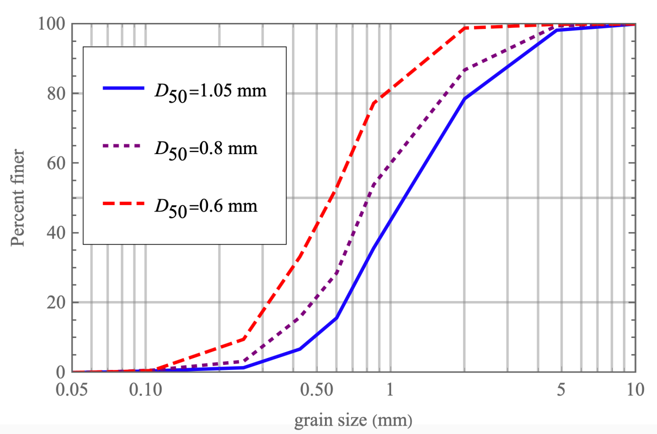

Figure 1. Particle size distributions for the graded samples

In Figure 2, the particle size distributions of the three samples presenting a graded distribution are shown. The sample with a D_{50} of 0.8 mm is the initial sand and the two others are obtained by changing the fraction (in terms of weight) of material from the different sieves.

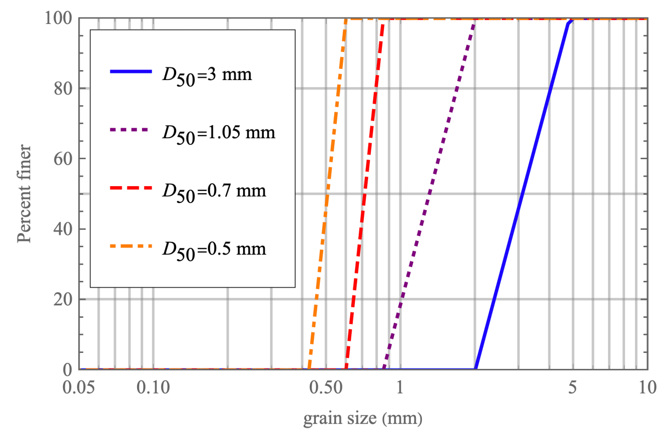

Figure 2. Particle size distributions for the uniform samples

For the samples presenting a uniform distribution shown in Figure 2, the grains obtained between two sieves from the initial sand are extracted to create the samples.

2.2. Triaxial setup

These different samples are then tested mechanically using a triaxial apparatus. All the samples have been tested with a confining pressure of 300 kPa in order to avoid grain breakage, and in dry conditions to avoid any chemical effects like pressure-solution that could affect the mechanical behavior and the shear band size. The samples are 140 mm in diameter and 70 mm in height and are loaded with a constant velocity of 2 mm/min. The cell used is transparent, which enables us to have a direct visual contact with the sample surrounded by a latex membrane. Three cameras have been placed around the cell and have been set to take pictures simultaneously every 30 seconds during the loading. A top view of the setup is shown in Figure 3. Speckles have been applied to the membrane using spray paint in order to create random patterns for the digital image correlation.

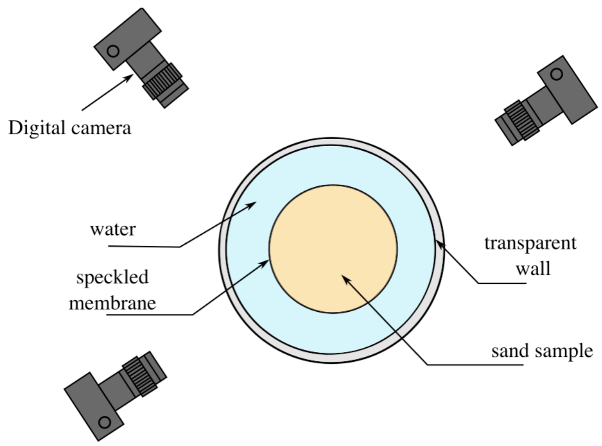

Figure 3. Top view of the experimental setup used to observe the shear band thickness during the triaxial tests using three cameras positioned at different angles.

2.3. Digital image correlation

The field of increment of displacement is measured using image analysis. For this methodology, images of the specimen are captured during the mechanical test at various stages of loading. Then, the pictures from the same point of view are analyzed using a numerical correspondence technique to identify the most similar patterns between successive images (see Figure 4 for an example of a picture and the field of incremental displacements associated). For this method to be efficient, the patterns must remain approximately constant between consecutive images and the local textural information be unique, that is why a random speckle pattern has been sprayed onto the membrane. The Matlab built-in function “normxcorr2” has been used to calculate the cross-correlation coefficients between images.

In these tests, even though pictures are taken from three angles, we apply the image correlation to the set of images from only one camera that has enabled to obtain the clearest view on the shear band. Moreover, the DIC is applied to a window at the center of the pictures (the red rectangle shown in Figure 4) to avoid refraction effects that are important on the sides of the sample (Bhandari, Powrie, and Harkness 2012) and to focus on a zone that is included inside the specimen all along the test.

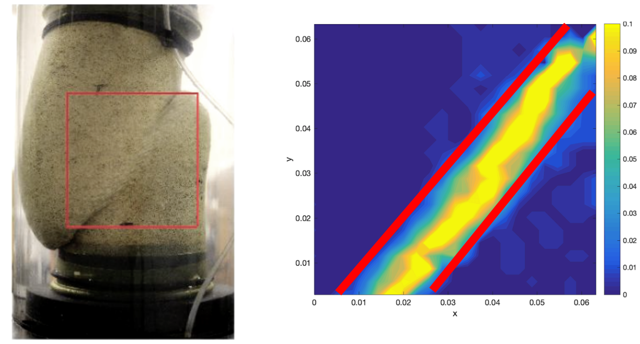

Figure 4. Picture taken from one of the cameras placed around the triaxial apparatus showing the shear band and the window (red) in which the DIC is applied (left). Map of deformation obtained from the DIC from the picture (right).

In order to estimate the shear band size, we calculate the increment of strain in the vertical direction ε_{11} as it is the largest one. Because the deformation between two subsequent images is approximately 0.7%, the assumption of small strain can be considered to calculate this increment. From the field of strain obtained in a 2D-plane, several sections in the x and y direction are considered to obtain the deformation $\varepsilon_{11}^{x}(x)$ or $\varepsilon_{11}^{y}(x)$ along these sections. A gaussian function is then used to interpolate the data for $\varepsilon_{11}^{x}(x)$ or $\varepsilon_{11}^{y}(y)$, as shown in Figure 5.

$$\varepsilon_{11}^{x}(x) = A^{x}\, e^{-\left(\frac{x-\mu^{x}}{\sigma^{x}}\right)^{2}}$$

$$\varepsilon_{11}^{y}(y) = A^{y}\, e^{-\left(\frac{y-\mu^{y}}{\sigma^{y}}\right)^{2}} \tag{1}$$

Where A^{i} is the amplitude, μ^{i} the mean and σ^{i} the standard deviation of the gaussian in the i-direction. This fitting formula gives us an objective way to measure the width of the zone of localized straining similar to the numerical analyses (Platt, Rudnicki, and Rice 2014; Rattez et al. 2018a). The width for a given section and direction is calculated as twice the root mean square width of the Gaussian:

$$w^{i} = 2\sqrt{2\ln(2)}\ \sigma^{i} \tag{2}$$

The actual width of the section is then calculated by:

$$w = \frac{w^{x}w^{y}}{\sqrt{(w^{x})^{2} + (w^{y})^{2}}} \tag{3}$$

Finally, the width for a given loading step is calculated as the mean of the width obtained from the different sections.

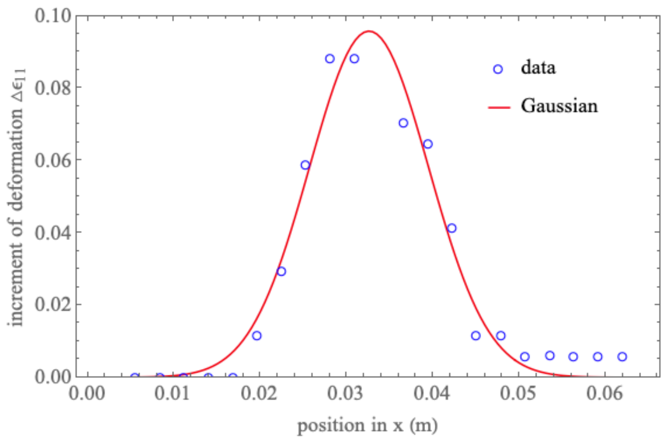

Figure 5. Example of increment of deformation along the x-axis obtained from the digital image correlation (points) and fitting with a gaussian distribution (solid line).

3. RESULTS

The mechanical tests we have performed have enabled us to obtain the stress-strain response of the samples together with the evolution of the shear band thickness.

In Figure 6, we show an example of the stress-strain response obtained for a sample presenting a uniform distribution and a mean grain size D_{50}=0.7 mm. The profiles of deformation obtained at different stages of the tests are also represented. We can observe the triggering of localization when the material reaches its peak value for the shear strength. The deformation localizes in a thinner zone during the weakening of the sample and tends toward a steady value at the end of the weakening phase.

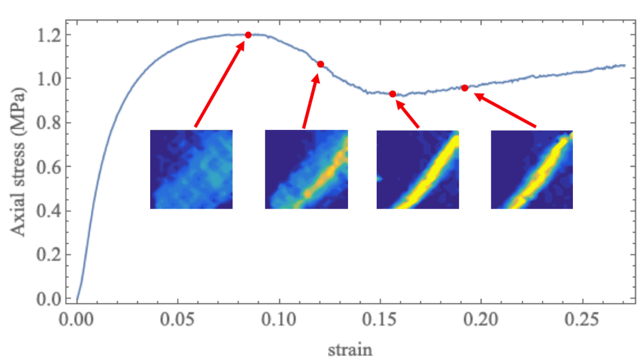

Figure 6. Example of stress-strain response obtained for a uniform distribution (D_{50}=0.7 mm) together with the deformation obtained from the DIC at different strains.

In Figure 7, the evolution of the shear band thickness obtained from the DIC and the fitting with a Gaussian function is shown for the same test as in Figure 6. It exhibits clearly the decrease of the shear band thickness and the steady value of the shear band obtained at the end of the weakening.

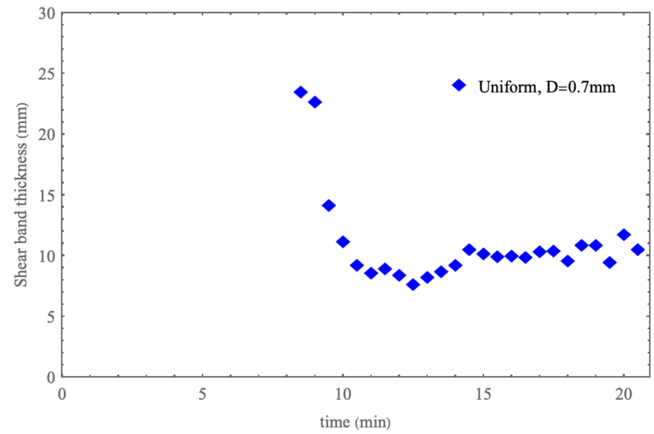

Figure 7. Example of the shear band thickness evolution with time assessed by the gaussian fitting for a uniform distribution (D_{50}=0.7 mm).

In Figure 8, we show the results of the shear band thickness for the uniform and graded particle size distributions as a function of the mean grain size of the distributions D_{50}. The gray zone corresponds to the area between the line 8*D_{50} and the line 18*D_{50}. We can observe that all the results lie in this zone, independently of the broadness of the distribution.

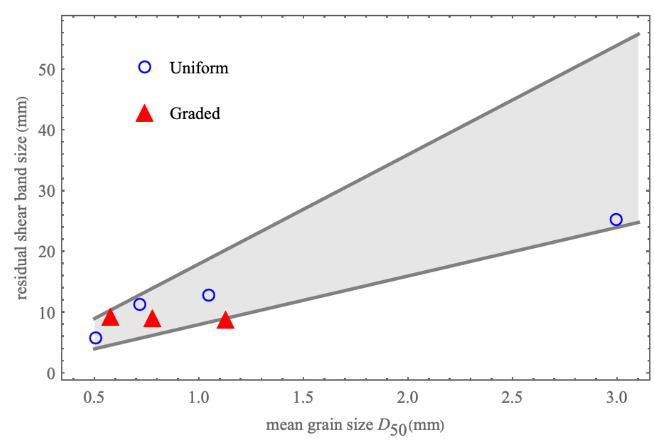

Figure 8. Residual shear band thickness obtained for the uniform and graded distribution as a function of the mean grain size.

4. CONCLUSIONS

Triaxial experiments have been conducted to investigate the influence of the particle size and the particle distribution on the shear band thickness at low confinements.

From the field of deformation obtained from the displacements of elementary cells identified on the membrane, the fitting of a gaussian distribution has enabled us to observe the evolution of the shear band size.

The shear band thickness exhibits a rapid decrease until reaching a residual value, which depends only on the mean grain size even for broad distributions.

The ratio of the residual thickness to the mean grain size D50 exhibits a value between 8 and 18 and this ratio is not influenced by a broader distribution. This tendency will be confirmed in future experiments performed on granular samples presenting a fractal particle size distribution.

ACKNOWLEDGEMENTS

This work was supported by the Southern California Earthquake Center (SCEC), award number 118062196. SCEC is funded by NSF Cooperative Agreement EAR-1033462 and USGS Cooperative Agreement G12AC20038.

REFERENCES

Bhandari, A. R., W. Powrie, and R. M. Harkness. 2012. "A Digital Image-Based Deformation Measurement System for Triaxial Tests." *Geotechnical Testing Journal* 35(2): 209–26.

Coop, M. R., K. K. Sorensen, T. Bodas Freitas, and G. Georgoutsos. 2004. "Particle Breakage during Shearing of a Carbonate Sand." *Geotechnique* 54(3): 157–63.

Dautriat, Jérémie et al. 2011. "Localized Deformation Induced by Heterogeneities in Porous Carbonate Analysed by Multi-Scale Digital Image Correlation." *Tectonophysics* 503(1–2): 100–116. http://dx.doi.org/10.1016/j.tecto.2010.09.025.

Desrues, Jacques et al. 2018. "How Does Strain Localise in Standard Triaxial Tests on Sand: Revisiting the Mechanism 20 Years On." *Mechanics Research Communications* 92(August): 142–46.

Desrues, Jacques, and Gioacchino Viggiani. 2004. "Strain Localization in Sand: An Overview of the Experimental Results Obtained in Grenoble Using Stereophotogrammetry." *International Journal for Numerical and Analytical Methods in Geomechanics* 28(4): 279–321.

Hill, R. 1962. "Acceleration Waves in Solids." *Journal of the Mechanics and Physics of Solids* 10(1): 1–16. http://linkinghub.elsevier.com/retrieve/pii/0022509662900248.

Hu, Manman, Manolis Veveakis, Thomas Poulet, and Klaus Regenauer-Lieb. 2017. "The Role of Temperature in Shear Instability and Bifurcation of Internally Pressurized Deep Boreholes." *Rock Mechanics and Rock Engineering*: 1–15.

Louis, Laurent, Teng Fong Wong, and Patrick Baud. 2007. "Imaging Strain Localization by X-Ray Radiography and Digital Image Correlation: Deformation Bands in Rothbach Sandstone." *Journal of Structural Geology* 29(1): 129–40.

Platt, John D, John W. Rudnicki, and James R. Rice. 2014. "Stability and Localization of Rapid Shear in Fluid-Saturated Fault Gouge : 2 . Localized Zone Width and Strength Evolution." *Journal of Geophysical Research: Solid Earth*.

Rathbun, Andrew P., and Chris Marone. 2010. "Effect of Strain Localization on Frictional Behavior of Sheared Granular Materials." *Journal of Geophysical Research* 115(B1): B01204. http://doi.wiley.com/10.1029/2009JB006466.

Rattez, Hadrien et al. 2018a. "Numerical Analysis of Strain Localization in Rocks with Thermo-Hydro-Mechanical Couplings Using Cosserat Continuum." *Rock Mechanics and Rock Engineering* 51(10): 3295–3311.

Rattez, Hadrien et al. 2018b. "The Importance of Thermo-Hydro-Mechanical Couplings and Microstructure to Strain Localization in 3D Continua with Application to Seismic Faults . Part II : Numerical Implementation and Post-Bifurcation Analysis." *Journal of the Mechanics and Physics of Solids* 115: 1–29.

Rattez, Hadrien, Fabrizio Disidoro, Jean Sulem, and Manolis Veveakis. 2019. "Influence of Dissolution on the Frictional Properties of Carbonate Faults." *Preprint EarthArXiv*.

Rattez, Hadrien, Ioannis Stefanou, and Jean Sulem. 2018. "The Importance of Thermo-Hydro-Mechanical Couplings and Microstructure to Strain Localization in 3D Continua with Application to Seismic Faults. Part I: Theory and Linear Stability Analysis." *Journal of the Mechanics and Physics of Solids* 115: 54–76.

Rattez, Hadrien, and Manolis Veveakis. 2020. "Weak Phases Production and Heat Generation Control Fault Friction during Seismic Slip." *Nature Communications* 11(350).

Rechenmacher, Amy L. 2006. "Grain-Scale Processes Governing Shear Band Initiation and Evolution in Sands." *Journal of the Mechanics and Physics of Solids* 54(1): 22–45. http://linkinghub.elsevier.com/retrieve/pii/S0022509605001481 (August 21, 2012).

Rechenmacher, Amy L., and Richard J. Finno. 2004. "Digital Image Correlation to Evaluate Shear Banding in Dilative Sands." *Geotechnical Testing Journal* 27(1): 13–22.

Rice, James R. 2006. "Heating and Weakening of Faults during Earthquake Slip." *Journal of Geophysical Research: Solid Earth* 111(5).

Rudnicki, John W., and James R. Rice. 1975. "Conditions for the Localization of Deformation in Pressure-Sensitive Dilatant Materials." *Journal of the Mechanics and Physics of Solids* 23(6): 371–94.

Segui, Carolina, Hadrien Rattez, and Manolis Veveakis. 2019. "On the Stability of Deep-Seated Landslides. The Cases of Vaiont (Italy) and Shuping (Three Gorges Dam, China)." *EarthArXiv preprint*.

Smith, Steven A. F., Stefan Nielsen, and Giulio Di Toro. 2015.

"Strain Localization and the Onset of Dynamic Weakening in Calcite Fault Gouge." *Earth and Planetary Science Letters* 413: 25–36. http://www.sciencedirect.com/science/article/pii/S0012821X14008048 (January 19, 2016).

Takano, Daiki, Nicolas Lenoir, Jun Otani, and Stephen A. Hall. 2015. "Localised Deformation in a Wide-Grained Sand under Triaxial Compression Revealed by X-Ray Tomography and Digital Image Correlation." *Soils and Foundations* 55(4): 906–15. http://dx.doi.org/10.1016/j.sandf.2015.06.020.

Vardoulakis, Ioannis. 2002. "Dynamic Thermo-Poro-Mechanical Analysis of Catastrophic Landslides." *Géotechnique* 52(3): 157–71.

Vardoulakis, Ioannis, and Jean Sulem. 1995. Library *Bifurcation Analysis in Geomechanics*. Glascow: Blackie.

Veveakis, Emmanuil, Ioannis Vardoulakis, and Giulio Di Toro. 2007. "Thermoporomechanics of Creeping Landslides: The 1963 Vaiont Slide, Northern Italy." *Journal of Geophysical Research: Earth Surface* 112(3): 1–21.

Zhang, Xiong, Lin Li, Gang Chen, and Robert Lytton. 2014. "A Photogrammetry-Based Method to Measure Total and Local Volume Changes of Unsaturated Soils during Triaxial Testing." *Acta Geotechnica* 10(1): 55–82.